Supporting Information

Highly conductive PANI/ATMP/$AgNO_3$ composite hydrogel electrodes for all-hydrogel-state supercapacitors

*Cheng Zhao[a], Shixiang Zhou[b], Jie Ma[a], Cong Liu[a], Jiading Zhu[a], Shifang Ye[a], Zhe Xin[a], Jiantao Cai[a], Peizhong Feng[a], Xueyu Tao[a]**

[a] School of Materials Science and Physics, China University of Mining and Technology, Xuzhou 221116, Jiangsu, China.

[b] Department of Materials Science and Engineering, National University of Singapore, 117575, Singapore.

* Corresponding author.

Email address: taoxueyu@cumt.edu.cn.

Characterization. Fourier transform infrared (FTIR) was recorded on a FTIR spectrophotometer (Thermo Nicolet IS5 Thermo Fisher, America). The morphology of prepared composite hydrogel electrode was examined by a scanning electron microscope (SEM, SU8220, Hitachi, Japan) at an acceleration voltage of 10 KV.

Electrochemical Measurements. The electrochemical behaviors of PPA-Ag composite hydrogel electrodes were tested in a three-electrode system on an electrochemical workstation (CHI660E, Shanghai, China). A platinum plate was used as a counter electrode and a calomel electrode was used as a reference electrode. Cyclic voltammetry (CV) curves were collected in the potential window of -0.2 to 0.8 V at the scan rates of 5, 10, 20, 30, 50, and 100 mV s^{-1}. The galvanostatic charge-discharge (GCD) measurements were taken with voltages ranging from -0.2 to 0.8 V at the current densities of 0.5, 1, 2, 3, and 5 A g^{-1}. Electrochemical impedance spectroscopy (EIS) was tested in the frequency range from 0.01 Hz to 100 kHz with an amplitude of 5 mV.

Specific capacitance of a single electrode can be calculated based on the data of CV (C_{mI}, F/g) and GCD (C_{mII}, F/g) by the following formula S1 and formula S2, respectively.

$$C_{mI} = \frac{\int Idv}{2 * Sr * m * \Delta U} \quad [S1]$$

$$C_{mII} = \frac{I\Delta t}{m\Delta U} \quad [S2]$$

Electronic conductivity was measured by four-probe method (Keithley 2000, Tektronix, America). The hydrogel sample was wrapped with four silver wires at equal distance. The electronic conductivity (σ) of hydrogel samples can be calculated by the

following formula S3.

$$\sigma = \frac{L}{R \times S} \quad [S3]$$

Where ***L*** (cm) is the distance between the silver wires, ***R*** (Ω) is the resistance of the hydrogel and ***S*** (cm^2) is the cross-sectional area of the hydrogel.

The electrochemical behaviors of PPA-Ag based supercapacitors were tested in a two-electrode system with voltage window of 0-1 V. Based on the data of GCD, specific capacitance (C_s, F/g) of assembled supercapacitors can be calculated by the following formula S4. Energy density (E_s, Wh/kg) and Power density (P_s, W/kg) were calculated according to the formula S5 and formula S6, respectively.

$$C_s = \frac{I\Delta t}{m\Delta V} \quad [S4]$$

$$E_s = \frac{C_{sa}\Delta U^2}{7.2} \quad [S5]$$

$$P_s = \frac{E_{sa} * 3600}{\Delta t} \quad [S6]$$

Where ***m*** (mg) is the mass load of hydrogel electrode, ***I*** (A) is the discharge current, Δ***t*** (s) is the discharge time, and Δ***U***(V) is the voltage window.

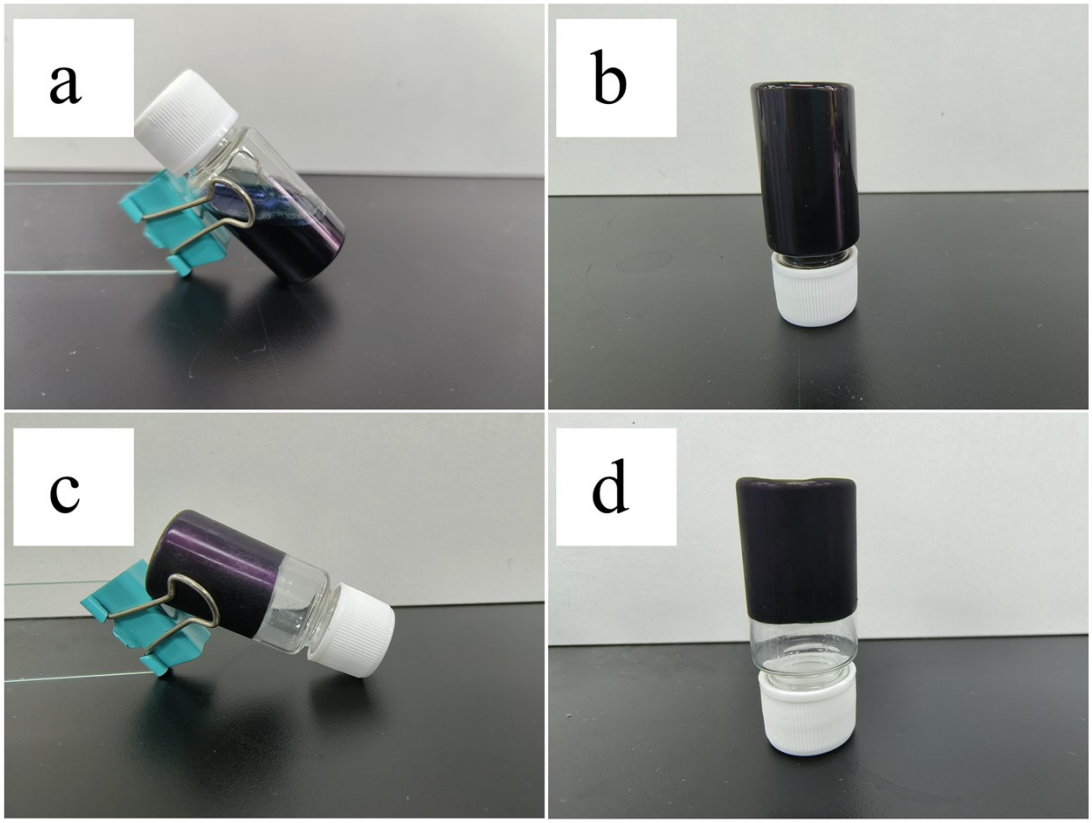

Fig. S1. Digital photos of PPA-Ag hydrogel (a) (b) before and (c) (d) after gelation.

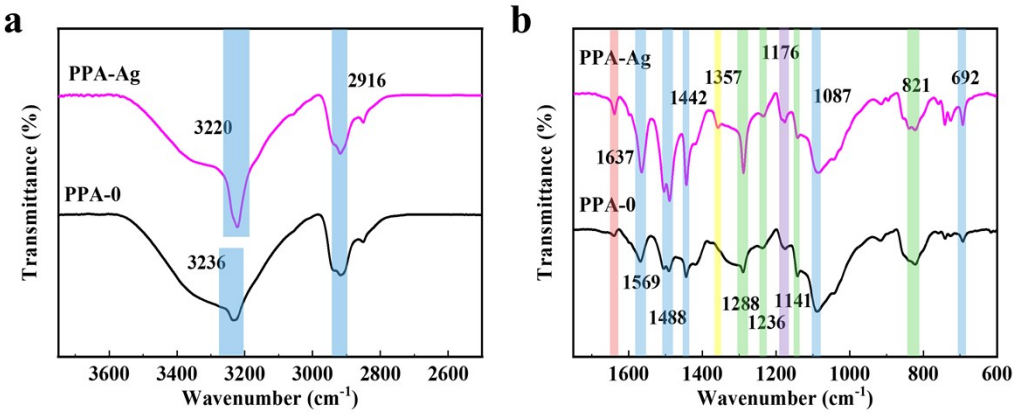

Fig. S2. FTIR spectra of PPA-0 and PPA-Ag composite hydrogels

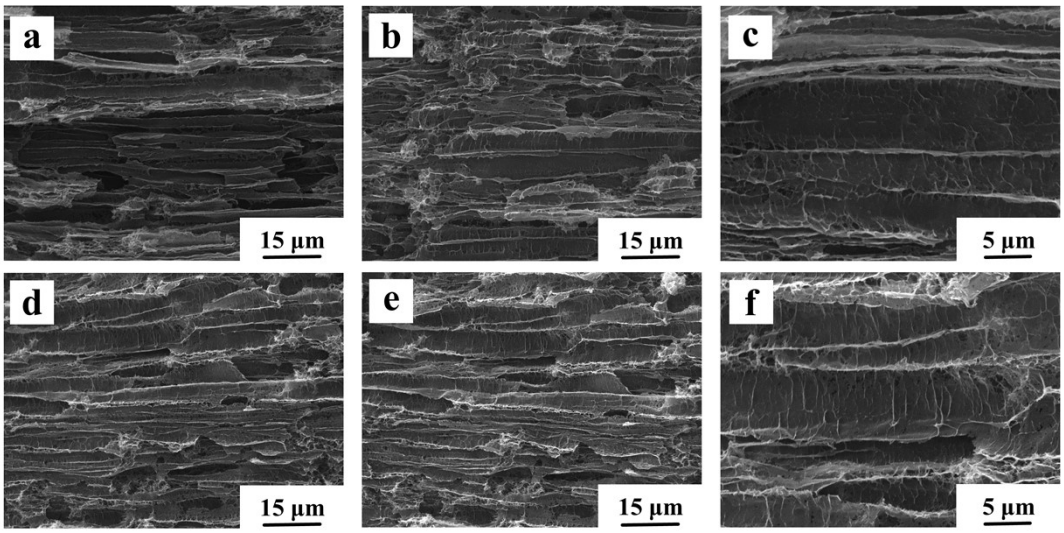

Fig. S3. SEM images from another cross-section that was perpendicular to the 3D porous-like cross-section: (a-c) PPA hydrogel; (d-f) PPA-Ag15 hydrogels.

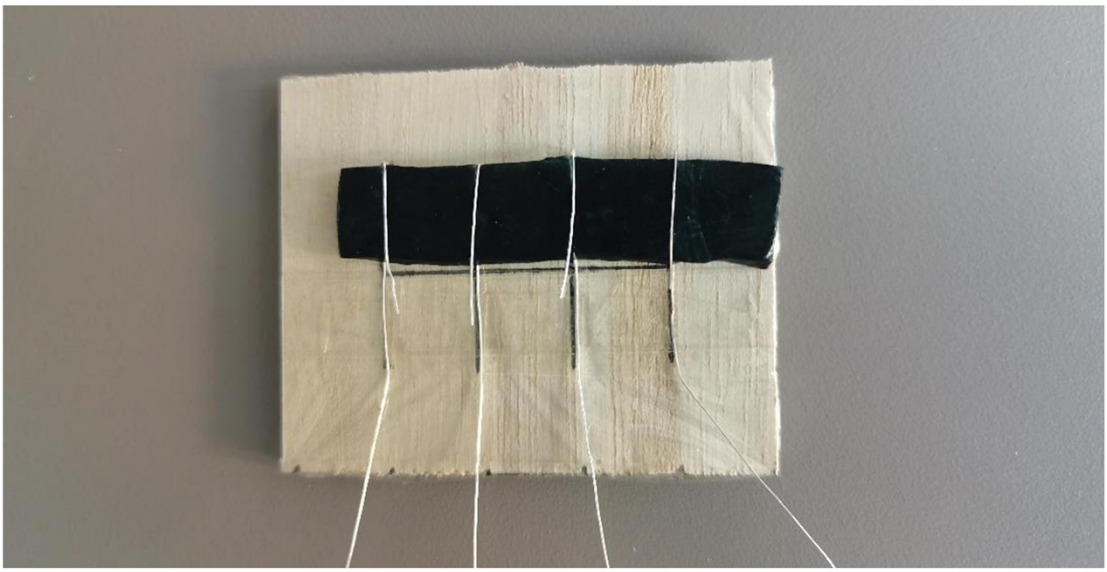

Fig. S4. Physical image of a four probe test gel sample

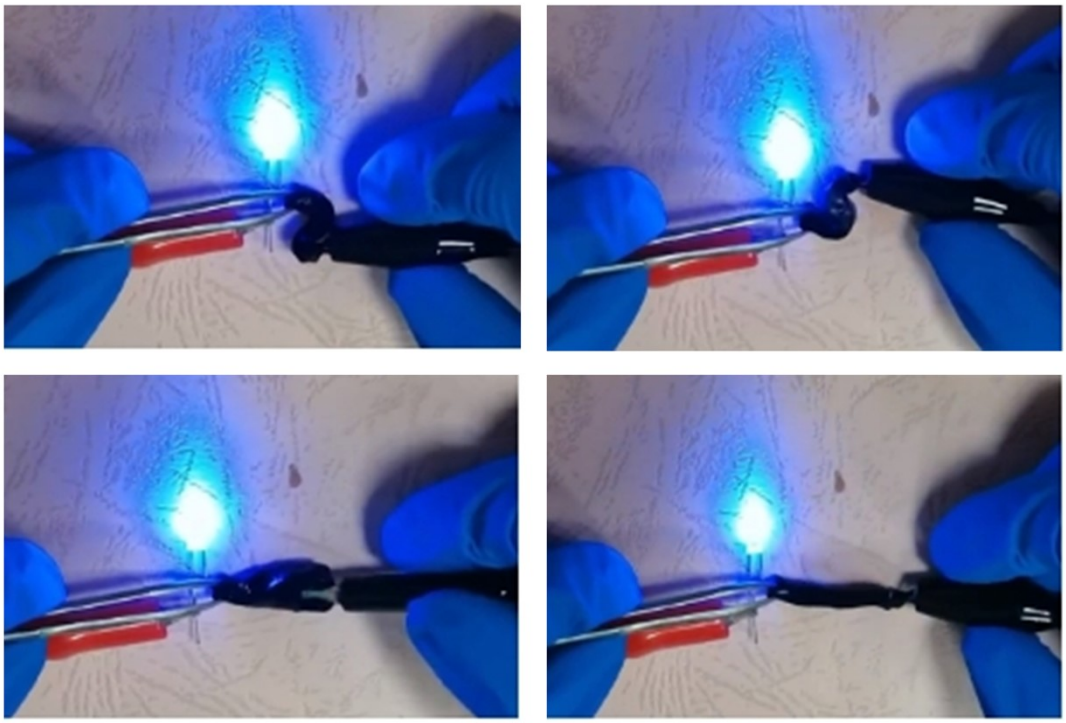

Fig. S5. Digital photos of PPA-Ag15 hydrogel as a conductor to light a LED.

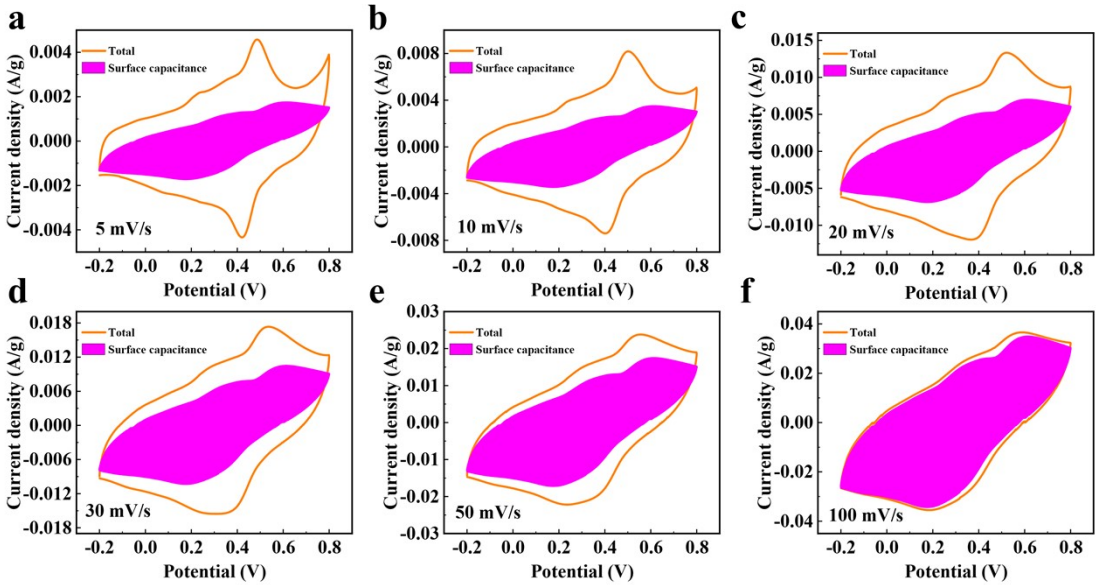

Fig. S6. CV curves of PPA-Ag15 hydrogel electrode measured at different scan rates, in which the shadowed area is the surface capacitive contribution.

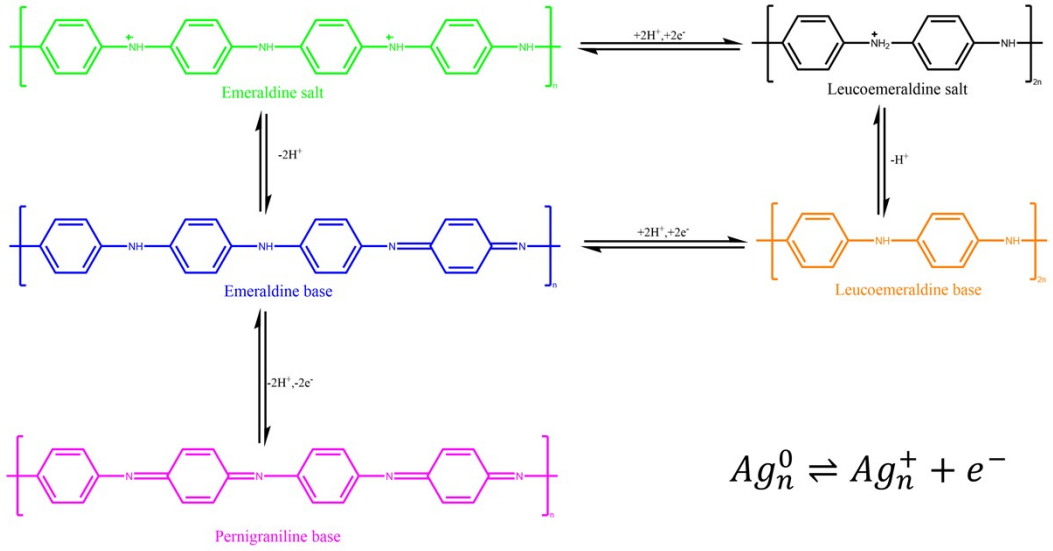

Fig. S7. Schematic diagram of redox transformation of polyaniline and Ag

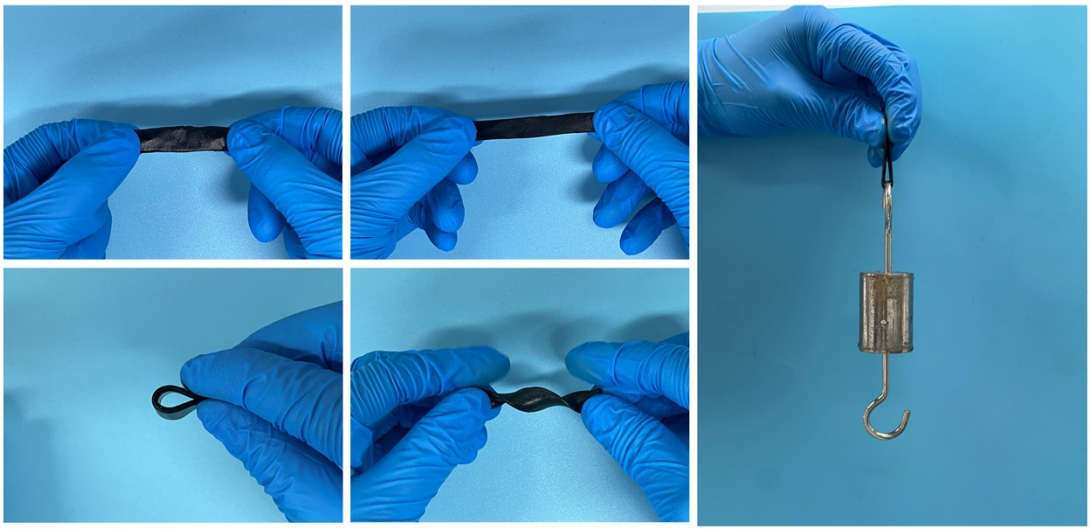

Fig. S8. Digital photos of PPA-Ag15 hydrogel under bending, twisting and holding a weight of 200 g.

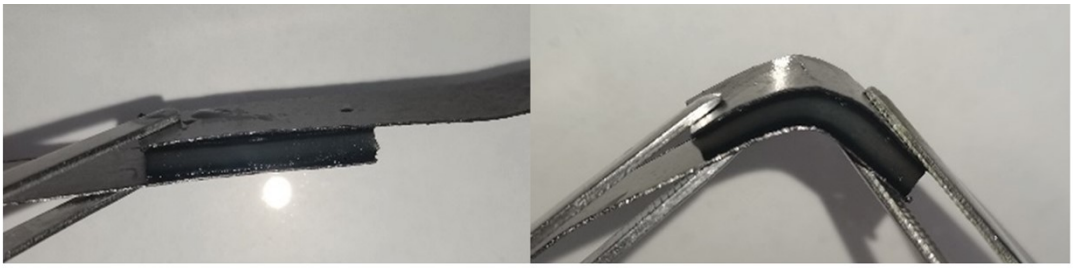

Fig. S9. Digital photographs of PPA-Ag hydrogel-based FSCs.

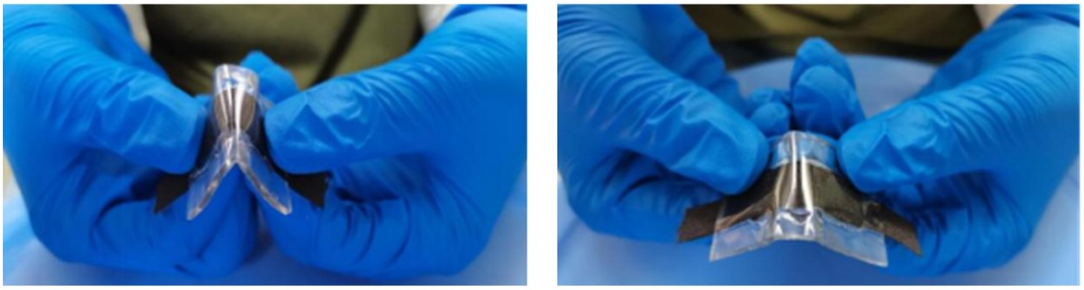

Fig. S10. Digital photographs of bent PPA-Ag hydrogel-based FSCs.

Table S1. Preparation of Conductive PPA-Ag Composite Hydrogels

	Solution A						Solution B	
	PVA	DI	PANI	ATMP	$AgNO_3$	wt%	DI	APS
PPA					0 mg	0		
PPA-Ag5					15.75 mg	0.05		
PPA-Ag10	1 g	10 mL	0.56 g	1.20 g	31.50 mg	0.1	5 mL	1.37 g
PPA-Ag15					47.25 mg	0.15		
PPA-Ag20					63.00 mg	0.2		

Table S2. The specific capacitance of the surface capacitive (C_s, F/g) and diffusion-controlled (C_d, F/g) response currents at different scan rates of PPA and PPA-Ag hydrogel electrodes.

Scan rate (mV/s)	PPA		PPA-Ag5		PPA-Ag10		PPA-Ag15		PPA-Ag20	
	C_s	C_d	C_s	C_d	C_s	C_d	C_s	C_d	C_s	C_d
5	121	179	135	193	149	201	169	235	158	203
10	121	168	135	169	149	176	169	214	158	179
20	121	135	135	124	149	130	169	168	158	133
30	121	104	135	90	149	93	169	129	158	97
50	121	63	135	49	149	51	169	78	158	54
100	121	14	135	13	149	14	169	18	158	16

Table S3. The specific capacitance (F/g) of PPA and PPA-Ag hydrogel electrodes calculated by GCD curves.

Current density (A/g)	PPA	PPA-Ag5	PPA-Ag10	PPA-Ag15	PPA-Ag20
0.5	317	442.5	467	510	493
1	290.6	416	418	460	449
2	270.6	387.6	395.4	429.8	420.2
3	258	371.7	379.8	413.4	403.8
5	236.5	346.5	350	389.5	381.5

Table S4. Resistance of PPA and PPA-Ag hydrogel electrodes.

Resistance	PPA	PPA-Ag5	PPA-Ag10	PPA-Ag15	PPA-Ag20
R_s	0.75	0.73	0.73	0.70	0.71
R_{ct}	1.72	1.43	1.33	1.12	1.17